Spectra in helical three-dimensional homogeneous isotropic turbulence

Vadim Borue and Steven A. Orszag
Fluid Dynamics Research Center, Princeton University, Princeton, New Jersey 08544-0710
(Received 6 February 1997)

Three-dimensional homogeneous isotropic turbulence with helicity is studied numerically at high Reynolds number. Helicity is generated by a large-scale white-in-time helical force. High Reynolds number is achieved by using hyperviscous dissipation. It is shown that a cascade of helicity from large to small scales develops. The scalings of the energy and helicity spectra are consistent with Kolmogorov inertial range scaling predictions. No inverse cascade of helicity is observed. [S1063-651X(97)09206-4]

PACS number(s): 47.27.Ak, 47.27.Gs, 47.27.Jv

I. INTRODUCTION

Helicity, the scalar product of velocity $\mathbf{v}$ and vorticity $\boldsymbol{\omega}$, is an inviscid invariant of three-dimensional homogeneous turbulence. It is known to play an important part in the generation of magnetic fields (see [1] for a review). In this paper we consider the influence of helicity on turbulence dynamics in the absence of a magnetic field. A recent general review of helical turbulent magnetic and nonmagnetic flows can be found in [2]. We introduce isotropic energy and helicity spectra $E(k)$ and $H(k)$ such that

$$\frac{1}{2}\langle \mathbf{v}^2 \rangle = \int_0^\infty E(k)\,dk \tag{1}$$

and

$$\langle \mathbf{v}\cdot\boldsymbol{\omega} \rangle = \int_0^\infty H(k)\,dk. \tag{2}$$

It may be shown that

$$|H(k)| \leqslant 2kE(k). \tag{3}$$

Since, in the inviscid limit, both energy and helicity are conserved, it was conjectured in [3] and extensively discussed in [4] that a simultaneous cascade of energy and helicity is possible. We consider the case when energy and helicity are injected by a white-in-time helical force at wave number k_f. If the energy injection rate is $\mathcal{E}$, then the helicity injection rate η satisfies the inequality $|\eta| \leqslant 2k_f\mathcal{E}$. The most straightforward scenario is a simultaneous cascade of both energy and helicity from large to small scales in which the helicity is carried linearly along with the energy cascade. In this case, dimensional considerations suggest that, using the Kolmogorov scaling [5] for $E(k)$,

$$E(k) = C_k \frac{\mathcal{E}^{2/3}}{k^{5/3}}, \tag{4}$$

then the helicity spectrum $H(k)$ satisfies

$$H(k) = C_h \frac{\eta}{\mathcal{E}^{1/3}k^{5/3}}. \tag{5}$$

The prediction (5) follows essentially from the fact that $H(k)$ should depend linearly on η. It is clear from Eqs. (4) and (5) that the relative helicity

$$\alpha(k) = \frac{H(k)}{2kE(k)} \tag{6}$$

decreases at small scales. Thus helicity scales essentially as a passive scalar [6] since it is dynamically unimportant at small scales. The decrease of the relative helicity at small scales was qualitatively predicted in [4].

Another hypothetical possibility [3] is that the presence of the mean helicity suppresses the direct cascade of energy from large to small scales and leads to an inverse cascade of energy to even larger scales while helicity itself cascades directly from large to small scales. It was shown in [7] that this possibility is inconsistent with Eulerian dynamics. The eddy-damped quasinormal Markovian (EDQNM) closure calculations in [4] also confirm that there is no inverse cascade in helical turbulence and that energy and helicity spectra scale according to Eqs. (4) and (5). Numerical simulations of helical three-dimensional decaying turbulence were carried out in [8]. Unfortunately, the low Reynolds number of these simulations does not permit the determination of quantitative scalings of energy and helicity spectra.

In previous works [9], we have already demonstrated that for a given numerical resolution we can effectively increase the extent of the inertial range of three-dimensional turbulence by an order of magnitude by using alternative forms of dissipation. We replace the normal Newtonian dissipation by a higher power of the Laplacian, i.e., a hyperviscosity. It was shown in [9] that three-dimensional inertial-range dynamics is relatively independent of the form of the hyperviscosity and that modest resolution simulations with high-order hyperviscosity lead to sufficiently extensive inertial ranges that measurement of a broad variety of otherwise intractable quantities can be made. Hyperviscosity is now a standard tool for numerical simulations of two-dimensional turbulence. The literature on the subject is extensive and too numerous to review here (see, e.g., [10] and references therein). For three-dimensional turbulence, hyperviscosity was used in [11] for simulations of stratified turbulence (hyperviscosity

was used concurrently with Newtonian viscosity to stabilize the calculations) and in [12] for simulations of rotating and decaying turbulence.

In this paper we address the question of scaling laws of the energy and helicity spectra in three-dimensional isotropic helical turbulence. We will demonstrate that in a statistically steady state where both the energy and helicity are injected by a white-in-time helical force at scale k_f both energy and helicity cascade from large to small scales with spectra that are consistent with Eqs. (4) and (5). No inverse cascade of energy or helicity is observed.

II. NUMERICAL RESULTS

The hyperviscosity-modified Navier-Stokes equations are

$$\partial_t v_i + v_j \partial_j v_i = -\partial_i p + (-1)^{h+1} \nu_h \Delta^h v_i + f_i, \tag{7}$$

where the pressure p is calculated from the incompressibility condition $\partial_i v_i = 0$. Vorticity is defined as $\omega_i = \varepsilon_{ijk} \partial_j v_k$, where ε_{ijk} is the antisymmetric tensor and the summation over repeated indices is assumed. On the right-hand side of Eq. (7) we include a white-noise-in-time Gaussian force that is nonzero only at some characteristic scale k_f:

$$\langle f_i(\mathbf{k},t) f_j(\mathbf{k}',t') \rangle \sim F_{ij}(\mathbf{k}) \delta(k^2 - k_f^2) \delta(\mathbf{k}+\mathbf{k}') \delta(t-t'), \tag{8}$$

and a hyperviscosity dissipation designed to provide an energy sink at small scales. The force injects both energy and helicity

$$F_{ij}(k) = \delta_{ij} - \frac{k_i k_j}{k^2} - i\beta \varepsilon_{ijl} \frac{k_l}{k}, \tag{9}$$

where $k = |\mathbf{k}|$. If the force (8) and (9) injects energy at the rate $\mathcal{E}$, the rate of helicity injection is $\eta = 2k_f \beta \mathcal{E}$. Therefore $|\beta| \leqslant 1$. The case $\beta = \pm 1$ corresponds to a maximally helical force. The helical force can be easily implemented numerically as

$$f_i(\mathbf{k}) = \left(\delta_{ij} - \frac{k_i k_j}{k^2} - i\gamma \varepsilon_{ijl} \frac{k_l}{k} \right) \xi_j \tag{10}$$

using Gaussian complex random variables with $\langle \xi_i \xi_j \rangle = 0$ and $\langle \xi_i \xi_j^* \rangle = \delta_{ij}$. The representation of the random force in Eq. (10) leads to a helical force with the tensor correlator structure (9) in which $\beta = 2\gamma/(1+\gamma^2)$ so that $|\beta| \leqslant 1$ is satisfied automatically.

We solve Eq. (7) using a pseudospectral parallel code [13]. We performed simulations with resolution 128^3 in a periodic box with size $L = 2\pi$ in each direction. The power h of the hyperviscous dissipation is chosen to maximize the extent of the inertial range. As in our previous work [9], we choose $h = 8$. For $h = 8$, the hyperviscous dissipation is nearly zero at wave numbers $k \leqslant N/3$ and abruptly turns on for $k \geqslant k_d \approx N/3$ (where N^3 is the numerical resolution). The hyperviscosity coefficient ν_h $(h = 8)$ for both the velocity and temperature equations is chosen so that $\nu_h (N/2)^{2h} \delta t \approx 0.5$, where δt is the time step of the numerical scheme. The time step, on the other hand, is fixed by the characteristic maximum velocity at large scales v_{max} by the Courant number criteria: $v_{max} \delta t N / 2\pi \leqslant 0.2$. Thus all parameters are uniquely defined by the large-scale flow and the numerical resolution. The Taylor microscale Reynolds number for this system may be defined as $R_\lambda \approx 50 (k_d/k_f)^{2/3}$, where k_d is the wave number where $k^2 E(k)$ is maximum ($k_d \approx 41$ for 128^3 numerical resolution).

We use only 128^3 numerical resolution since the Reynolds number dependence of the energy spectrum has been studied by us previously [9] and we expect that the Reynolds number dependence of the helicity spectrum is similar to that of the energy spectrum. Moreover, it follows that the total helicity is a strongly fluctuating, not positive-definite, quantity since a long total integration time is required to get meaningful results. The use of 256^3 numerical resolution is still computationally quite expensive; we do not expect any new helicity specific physics to emerge at higher Reynolds number and the present 128^3 resolution, which is, we believe, big enough to verify basic concepts and allows us to explore a sufficiently broad range of parameters.

We start our numerical investigation by considering the maximally helical force with $\beta = \gamma = 1$ that acts only at the largest scales, i.e., on wave-number shells $k_f = 1,2$. We measure wave numbers in $2\pi/L = 1$ units. The time scale of the problem is set by an amplitude of the force (8) that is chosen so that the characteristic velocity $v_0 \propto (\mathcal{E}L)^{1/3} = 1$ and the characteristic time scale $t_0 = L/2\pi v_0 = 1$. The characteristic vorticity is $\omega_0 = 2\pi v_0 / L = 1$ and the characteristic helicity is $h_0 = v_0 \omega_0$. We characterize the global behavior of the flow by a time-dependent root-mean-square velocity, vorticity, and helicity defined as

$$v_{rms} = \frac{1}{\sqrt{3}} \langle \boldsymbol{v}^2 \rangle^{1/2}, \quad \omega_{rms} = \frac{1}{\sqrt{3}} \langle \boldsymbol{\omega}^2 \rangle^{1/2}, \quad h = \langle \boldsymbol{v} \cdot \boldsymbol{\omega} \rangle, \tag{11}$$

respectively. The averaging in Eqs. (11) is carried out only in space. Flow in a periodic box is an open flow and is characterized by strong large-scale intermittency [9]. The signals for $v_{rms}(t)$, $\omega_{rms}(t)$, and $h(t)$ obtained during the total integration time are shown in Fig. 1. It is evident from Fig. 1 that helicity is a more intermittent quantity than the large-scale velocity.

For helical homogeneous isotropic three-dimensional turbulence, velocity spectra consistent with the definitions (1) and (2) have the tensor structure

$$\langle v_i(\boldsymbol{k}) v_j(-\boldsymbol{k}) \rangle = \left(\delta_{ij} - \frac{k_i k_j}{k^2} \right) \frac{E(k)}{4\pi k^2} - i \varepsilon_{ijl} \frac{k_l}{k^2} \frac{H(k)}{8\pi k^2}. \tag{12}$$

It is instructive to demonstrate the existence of energy and helicity cascades from large to small scales. We define the energy (helicity) flux as

$$J_{E(h)}(k) = \int_{k'>k}^{\infty} T_{E(h)}(k') dk', \tag{13}$$

where the isotropic energy (helicity) transfer function $T_{E(h)}(h)(k)$ equals

$$T_{E(h)}(\boldsymbol{k}) = \int N_{E(h)}(\boldsymbol{p}) 2k \delta(\boldsymbol{p}^2 - k^2) d\boldsymbol{p}, \tag{14}$$

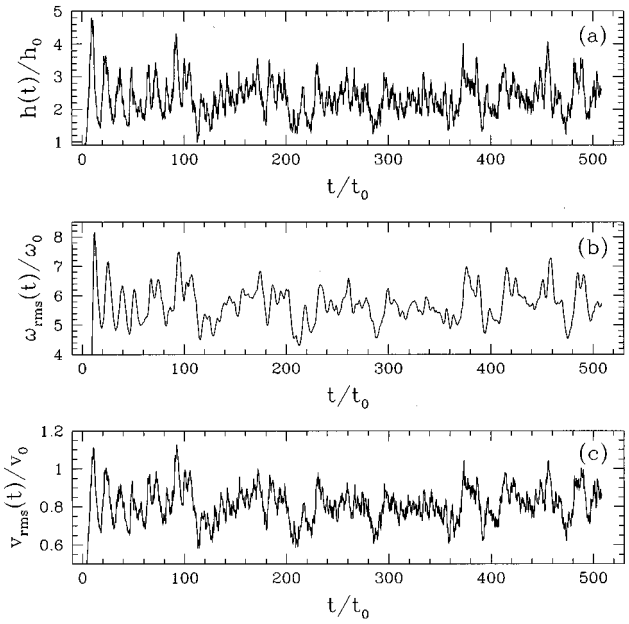

FIG. 1. Time series averaged in space: (a) mean helicity $h(t)/h_0$, (b) $\omega_{rms}(t)/\omega_0$, and (c) $v_{rms}(t)/v_0$. Time, velocity, vorticity, and helicity are measured in units of t_0, v_0, ω_0, and h_0, respectively.

with

$$N_E(\boldsymbol{k}) = -\langle v_i(\boldsymbol{k})[v_j \partial_j v_i](-\boldsymbol{k})\rangle \tag{15}$$

in the case of the energy flux and with

$$N_h(\boldsymbol{k}) = -2\langle \omega_i(\boldsymbol{k})[v_j \partial_j v_i](-\boldsymbol{k})\rangle \tag{16}$$

in the case of the helicity flux.

We have verified directly that the velocity spectra indeed have the structure (12) consistent with isotropy. The isotropic energy spectrum $E(k)$ and the energy flux $J_E(k)$ for the case of maximal helicity force are plotted in Fig. 2. The energy spectrum is scaled to verify the scaling law (4). The spectrum and the energy flux are nearly identical to the ones observed by us previously [9] in the case of homogeneous isotropic turbulence driven by a white-in-time force. As in the case of nonhelical isotropic turbulence, there is the bottleneck part of the spectrum near the dissipation cutoff k_d [9]. In both cases the scaling of the energy spectrum slightly deviates from the Kolmogorov law (4). These small deviations were extensively discussed by us earlier. We think that these deviations probably reflect the fact that, although the energy spectrum is globally isotropic, at each given moment of time it is anisotropic. Only after substantial averaging is global isotropy recovered. If we should expect the Kolmogorov scaling law to hold only at scales that are locally isotropic regardless of global anisotropy, we need about a decade of scales to reach this state of local isotropy. Therefore, although the system is formally globally isotropic, it is locally isotropic starting only from $k \approx 7-10$ [9]. Thus we believe that any small deviations from the Kolmogorov law reflect the fact that the system is locally anisotropic at large scales. However, there is a possibility that these deviations are real.

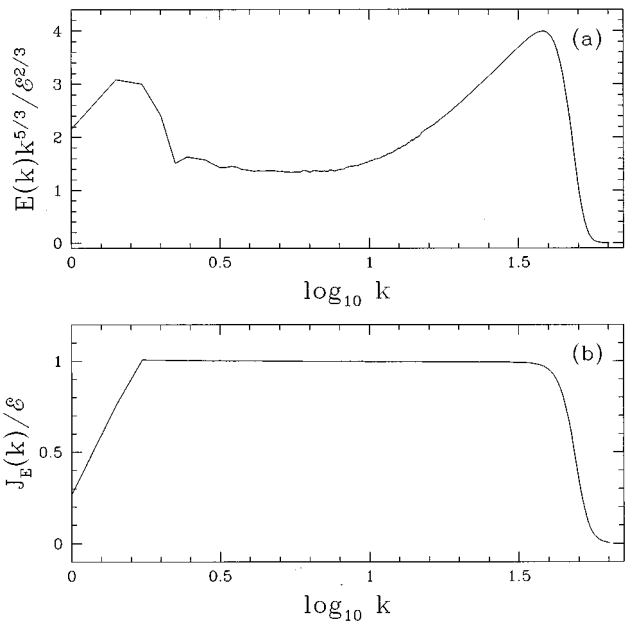

FIG. 2. (a) Scaled energy spectrum $E(k)k^{5/3}/\mathcal{E}^{2/3}$ and (b) scaled energy flux $J_E(k)/\mathcal{E}$ as functions of $\log_{10}k$.

The isotropic helicity spectrum $H(k)$ and the helicity flux for this case of maximal helicity force are plotted in Fig. 3; those results show that the helicity spectrum exhibits a bottleneck phenomenon similar to that of the energy spectrum. It is interesting to note that a bottleneck part in both the energy and helicity spectra was also observed in the EDQNM closure in [4]. $H(k)$ approximately satisfies the Kolmogorov law (5). There are also small deviations from the Kolmogorov law as in the case of the energy spectrum; again, small deviations could be local anisotropy. A constant helicity flux from large to small scales can be observed. It is

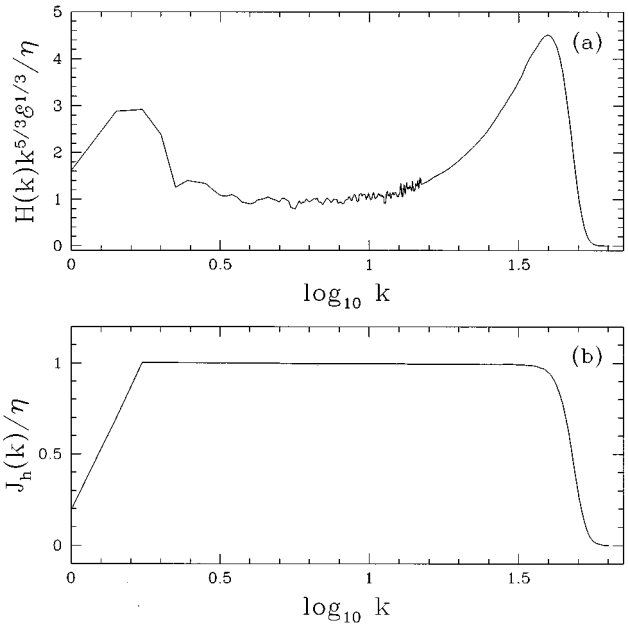

FIG. 3. (a) Scaled helicity spectrum $H(k)k^{5/3}\mathcal{E}^{1/3}/\eta$ and (b) scaled energy flux $J_E(k)/\mathcal{E}$ as functions of $\log_{10}k$.

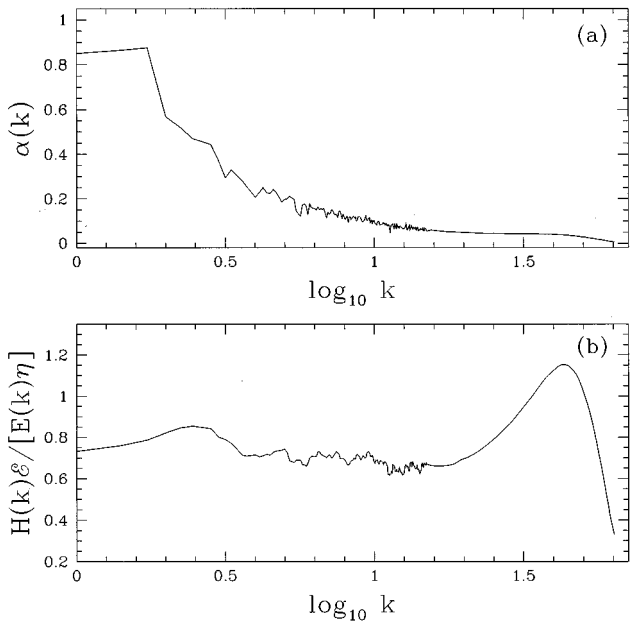

FIG. 4. (a) Relative helicity $\alpha(k)$ and (b) ratio $H_E(k)\mathcal{E}/E(k)\eta$ as functions of $\log_{10}k$.

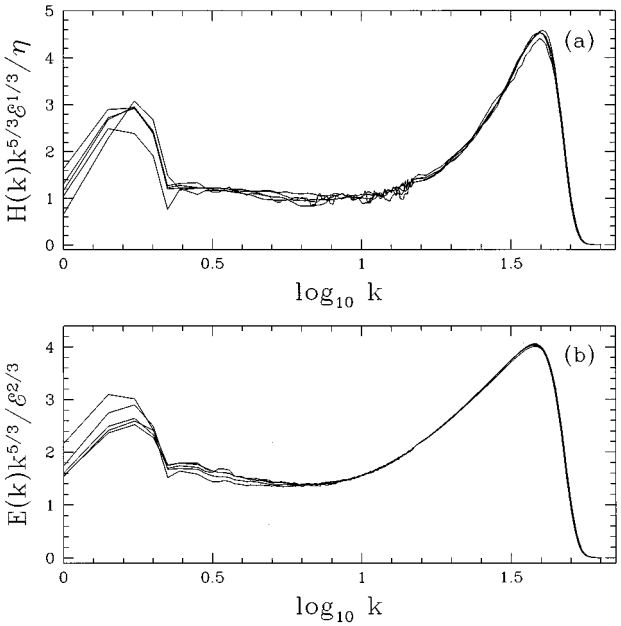

FIG. 5. (a) Scaled energy spectra $E(k)k^{5/3}/\mathcal{E}^{2/3}$ and (b) scaled helicity spectra $H(k)k^{5/3}\mathcal{E}^{1/3}/\eta$ as functions of $\log_{10}k$. Spectra are obtained for different levels of mean helicity $\beta=0.15,0.35,0.55,0.75,1$ and are superimposed.

interesting to compare Kolmogorov constants for the energy and the helicity spectra C_k and C_h, respectively, with the values obtained using EDQNM closure [4]. In our simulation, we find $C_K\approx1.4$ and $C_h\approx1$. According to the EDQNM closure, $C_K\approx1.4$ and $C_h\approx2.23$. Therefore, if the value of C_K is in good agreement with the EDQNM closure, the value of C_h exhibits substantial deviation from it. Qualitatively, the scenario that the linear helicity cascade is similar to the case of a passive scalar discussed in [3,4] is quite well satisfied according to our data.

It is interesting to calculate also the relative helicity $\alpha(k)$ (6) and the ratio of the helicity and energy spectra $H_E(k)\mathcal{E}/[E(k)\eta]$, which are plotted in Fig. 4. As can be seen from Fig. 4, at large scales, the velocity field is nearly maximally helical and the relative helicity decays as $\sim1/k$ at large wave numbers. The ratio of the helicity to the energy spectrum is approximately constant, except in the dissipation range. The value of this constant ≈0.7 is surprisingly close to the corresponding quantity for a passive scalar or for homogeneous convection [14], where this ratio is called the effective (turbulent) Prandtl number.

The scenario of a linear helicity cascade carried alongside the energy cascade requires that $H(k)$ depends linearly on η. We can easily check this dependence by carrying out simulations with variable levels of helicity by tuning the parameter γ in the force (10). We have performed runs for the helical forcing at the same k_f as for the case of a maximally helical force ($\gamma=1$) with $\gamma\approx0.075,0.185,0.3,0.45$ corresponding, according to Eq. (8), to helicity level $\beta\approx0.15,0.35,0.55,0.75$. We verified that, for these runs, $\eta/\mathcal{E}\propto\beta=2\gamma/(1+\gamma^2)$. In Fig. 5 we plot energy and helicity spectra for different levels of injected helicity. Energy (helicity) spectra are superimposed and scaled in order to check the Kolmogorov scalings for energy (4) and helicity (5). It is clear from the results plotted in Fig. 5 that the energy spectrum is nearly independent of the mean helicity level in the system. Also the helicity spectra are indeed linearly proportional to the helicity injection rate η. The scatter in the helicity spectra for lower levels of helicity is more pronounced since relative fluctuations of the helicity increase as the level of mean helicity decreases. The higher level of fluctuations at smaller wave numbers are caused by our measurement procedure in which isotropic spectra are measured using substantially thinner shells at low wave numbers (this being necessary to avoid systematic errors in representing isotropic spectra by a histogram with bins that are too thick at low wave numbers).

To check the possibility of inverse energy or helicity cascades as suggested in [3] we made several runs with the helical force at intermediate scales $k_f\approx10$. No inverse energy or helicity cascade was observed. Both energy and helicity cascade from the scale of injection toward small scales leading to constant energy and helicity fluxes from large to small scales. This conclusion agrees with the same conclusion reached within the framework of EDQNM closure [4].

III. DISCUSSION

The main conclusion of this paper is that helicity apparently does not play a significant role in the cascade of energy from large to small scales. Helicity is inherently a large-scale quantity. When helicity is injected at large scales, it is transferred to small scales by the energy cascade. In this sense, helicity behaves similarly to a passive scalar. Helicity spectra depend linearly on the level of helicity injection and scale similarly to spectra of a passive scalar in accord with the Obukhov-Corrsin hypothesis [6]. Relative helicity decreases at small scales; even if helicity could play some significant

dynamic role at the largest anisotropic scales of the system, its role would decrease at small scales where the turbulence dynamics become more universal. No inverse helicity or energy cascade has been observed. Although the presence of mean helicity may be unimportant for the dynamics of the energy cascade, the situation changes drastically in the case of magnetohydrodynamics. In a magnetic fluid, the presence of a small-scale kinetic helicity leads to magnetic helicity production that cascades toward large scales, leading eventually to large-scale magnetic-field generation through the dynamo effect. We hypothesize that information on the dynamics of kinetic helicity in the absence of a magnetic field as given here can help to understand the more complicated kinetic helicity dynamics in magnetohydrodynamics.

ACKNOWLEDGMENTS

We are grateful to V. Yakhot for valuable discussions. This research was performed in part using the CSCC parallel computer system operated by Caltech on behalf of the Concurrent Supercomputing Consortium. Access to this facility was provided by DARPA. The computations have been performed on the Intel Delta at Caltech and on the IBM PVS at Princeton. This work was supported by DARPA/ONR under Contract No. N00014-92-J-1796.

[1] H.K. Moffat, *Magnetic Field Generation in Electrically Conducting Fluids* (Cambridge University Press, Cambridge, 1978).
[2] H.K. Moffat and A. Tsinober, Annu. Rev. Fluid Mech. **24**, 281 (1992).
[3] A. Brassaud, U. Frisch, J. Leorat, M. Lesieur, and A. Mazure, Phys. Fluids **16**, 1366 (1973).
[4] J.C. André and M. Lesieur, J. Fluid Mech. **81**, 187 (1977).
[5] A.N. Kolmogorov, C. R. Acad. Sci. URSS **30**, 301 (1941).
[6] A.M. Obukhov, Izv. Akad. Nauk SSSR **30**, 311 (1949); S. Corrsin, J. Appl. Phys. **22**, 469 (1951).
[7] R.H. Kraichnan, J. Fluid Mech. **59**, 745 (1973).
[8] W. Polifke and L. Shtilman, Phys. Fluids A **1**, 2025 (1989).
[9] V. Borue and S.A. Orszag, Europhys. Lett. **29**, 687 (1995); Phys. Rev. E **52**, R856 (1995); **53**, R21 (1996); J. Fluid Mech. **306**, 293 (1996).
[10] V. Borue, Phys. Rev. Lett. **71**, 3967 (1993).
[11] J.R. Herring and O. Metais, J. Fluid Mech. **202**, 97 (1989).
[12] P. Bartello, O. Metais, and M. Lesieur, J. Fluid Mech. **273**, 1 (1994).
[13] E. Jackson, Z.-S. She, and S. Orszag, J. Sci. Comput. **6**, 27 (1991).
[14] V. Borue and S.A. Orszag (unpublished).